Electronic Supplementary Information

Electrochemical *meso*-Functionalization of Magnesium(II) Porphine†

Charles H. Devillers,* Abdou K. D. Dime, Hélène Cattey and Dominique Lucas*
Institut de Chimie Moléculaire de l'Université de Bourgogne, UMR CNRS 5260, Université de Bourgogne, BP 47870, 21078 DIJON Cedex, France.
E-mail: charles.devillers@u-bourgogne.fr; dominique.lucas@u-bourgogne.fr

Contents

Experimental Details

Synthesis

Magnesium porphine **1** was synthesized according to known procedures.[1] Data (^{1}H NMR, ^{13}C NMR, UV-Visible absorption, and MALDI-TOF mass spectrum) were consistent with those obtained in reference [1].

Materials

Pyridine (VWR-BDH-Prolabo, 99.90% on anhydrous product), PPh_3 (Fluka, puriss., >99%), tetraethylammonium hexafluorophosphate ($TEAPF_6$, Fluka puriss., electrochemical grade, ≥99.0%), *2,6*-lutidine (Aldrich, purified by redistillation, ≥99%) and MeOH (Sigma-Aldrich, Chromasolv for HPLC, min. 99.9%) were used as received. Tetra-*n*-butylammonium hexafluorophosphate ($TBAPF_6$) was synthesized by mixing stoichiometric amounts of tetra-*n*-butylammonium hydroxide (Alfa-Aesar, 40% w/w aq. sol.) and hexafluorophosphate acid (Alfa-Aesar, ca 60% w/w aq. sol.). After filtration, the salt was recrystallized three times in ethanol and dried at 80 °C during at least two days. CH_2Cl_2 (Carlo Erba 99.5%) and CH_3CN (SDS, Carlo Erba, HPLC gradient 99.9%) were distilled from P_2O_5 and CaH_2 respectively.

Electrochemistry

All manipulations were performed using Schlenk techniques in an atmosphere of dry oxygen-free argon at room temperature (T = 20°C ± 3°C). The supporting electrolyte was degassed under vacuum before use and then dissolved to a concentration of 0.1 mol L^{-1}. Voltammetric analyses were carried out in a standard three-electrode cell, with an EG & G Princeton Applied Research (PAR) Model 273 potentiostat, connected to an interfaced computer that employed Electrochemistry Power Suite software. The reference electrode was a saturated calomel electrode (SCE) separated from the analysed solution by a sintered glass disk filled with the background solution. The auxiliary electrode was a platinum wire separated from the analysed solution by a sintered glass disk filled with the background solution. For all voltammetric measurements, the working electrode was a platinum electrode (*Ø* = 2 mm). In these conditions, when operating in pyridine (0.1 M $TBAPF_6$), the formal potential for the ferrocene (+/0) couple was found to be +0.55 V *vs.* SCE. When operating in a mixture of CH_2Cl_2/CH_3CN 4/1 (0.1 M $TEAPF_6$) the formal potential for the ferrocene (+/0) couple was found to be +0.40 V *vs.* SCE.

Bulk electrolyses were performed in a cell with three compartments separated with glass frits of medium porosity with an Amel 552 potentiostat coupled with an Amel 721 electronic integrator. A platinum wire spiral (*l* = 53 cm, *Ø* = 1 mm) was used as the working electrode, a platinum plate as the counter electrode and a saturated calomel electrode as the reference electrode. The electrolysis was followed by TLC and UV-visible absorption measurements and was stopped when the pink spot corresponding to **1** disappeared on TLC and when UV-visible absorption spectra and current did not evolve anymore. For pyridinium substitution, 2.0 ± 0.1 faraday per mol of **1** were necessary to exhaust totally the starting product. For the triphenylphosphonium substitution, 3.4 ± 0.2 faraday per mol of **1** were used.

Work-up procedures

2^+,PF_6^-:

After electrolysis in pyridine, work-up involved evaporating the red solution mixture to dryness under reduce pressure. The resulting crude solid was dissolved in a minimum of cold (*ca*. −90 °C) MeOH and the precipitated supporting electrolyte was removed by filtration and washed with cooled MeOH. The red filtrate was evaporated to dryness and this precipitation/filtration procedure was repeated one more time. The crude product was then purified by column chromatography (SiO_2, 0 to 2% MeOH, 1% pyridine in CH_2Cl_2). The first light pink fraction was unreacted **1** (< 1 mg). The second red fraction corresponded to **2^+,PF_6^-**.

3^+,PF_6^-:

The work-up involved evaporating the blue/green solution mixture to dryness under reduce pressure. The resulting crude solid was dissolved in a minimum of CH_2Cl_2 and this solution was washed four times with 250 mL of distilled water to remove the supporting electrolyte. The blue/green organic phase was evaporated to dryness. The crude product was then purified by column chromatography (Alumina, 0 to 1% MeOH in CH_2Cl_2). The first colourless fraction was unreacted PPh_3, the second blue/purple fraction was **3^+,PF_6^-**.

Instruments

UV-visible absorption spectra were obtained with a Varian UV-vis spectrophotometer Cary 50 scan using quartz cells (Hellma).

Mass spectra were obtained on a Bruker ProFLEX III spectrometer (MALDI-TOF) using dithranol as matrix.

NMR spectra were measured on a BRUKER 600 MHz Avance II spectrometer. The reference was the residual non-deuterated solvent (CH_3COCH_3 or CH_3OH).

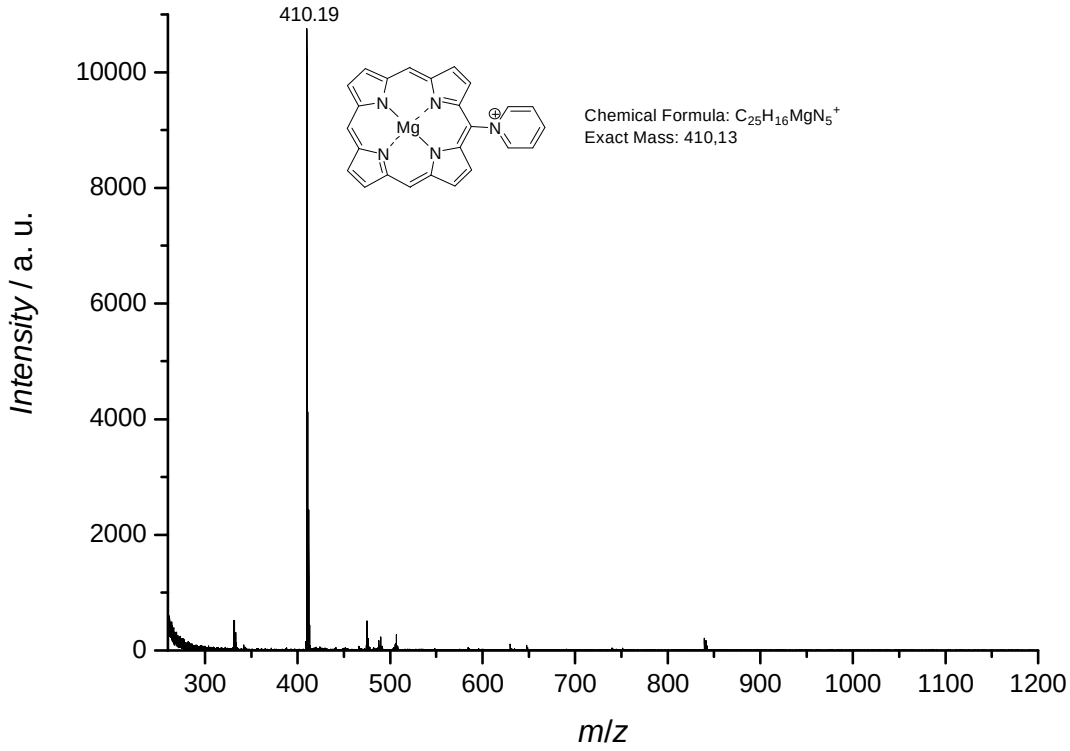

Fig. 1 MALDI-TOF mass spectrum of the crude solution resulting from the electrolysis of **1** in pyridine 0.1 M $TBAPF_6$; E_{app} = 0.72 V *vs*. SCE, −2 e, working electrode: Pt spiral.

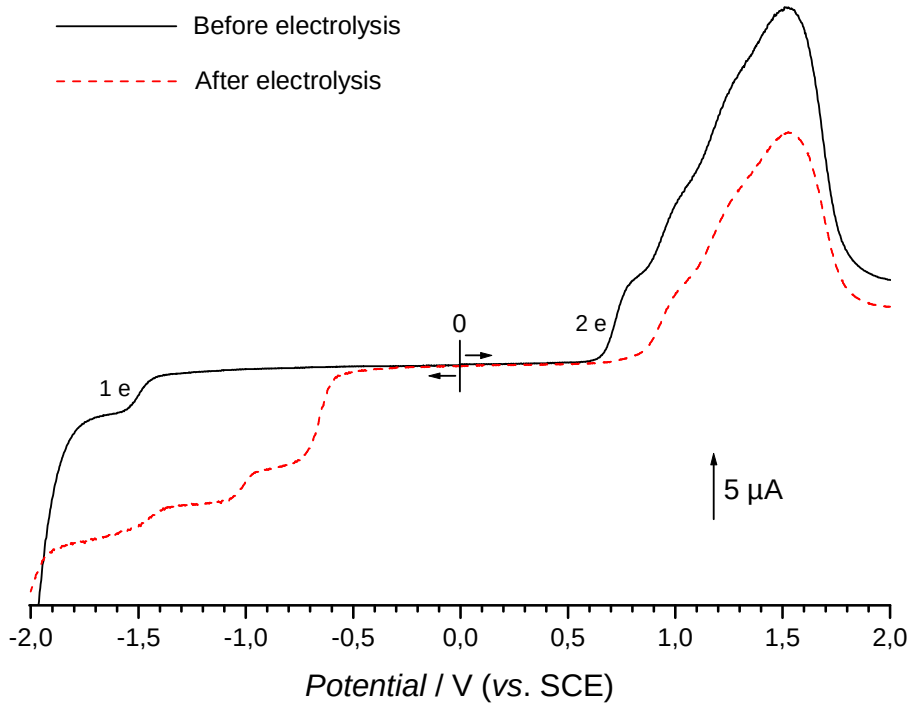

Fig. 2 RDE voltammogram before (black/solid line) and after (red/dashed line) electrolysis of **1** in pyridine containing 0.1 M $TBAPF_6$ (WE: Pt, $\varnothing$ = 2 mm, 10 mV s^{-1}, ω = 500 rpm, [**1**] = 5.0×10^{-4} M).

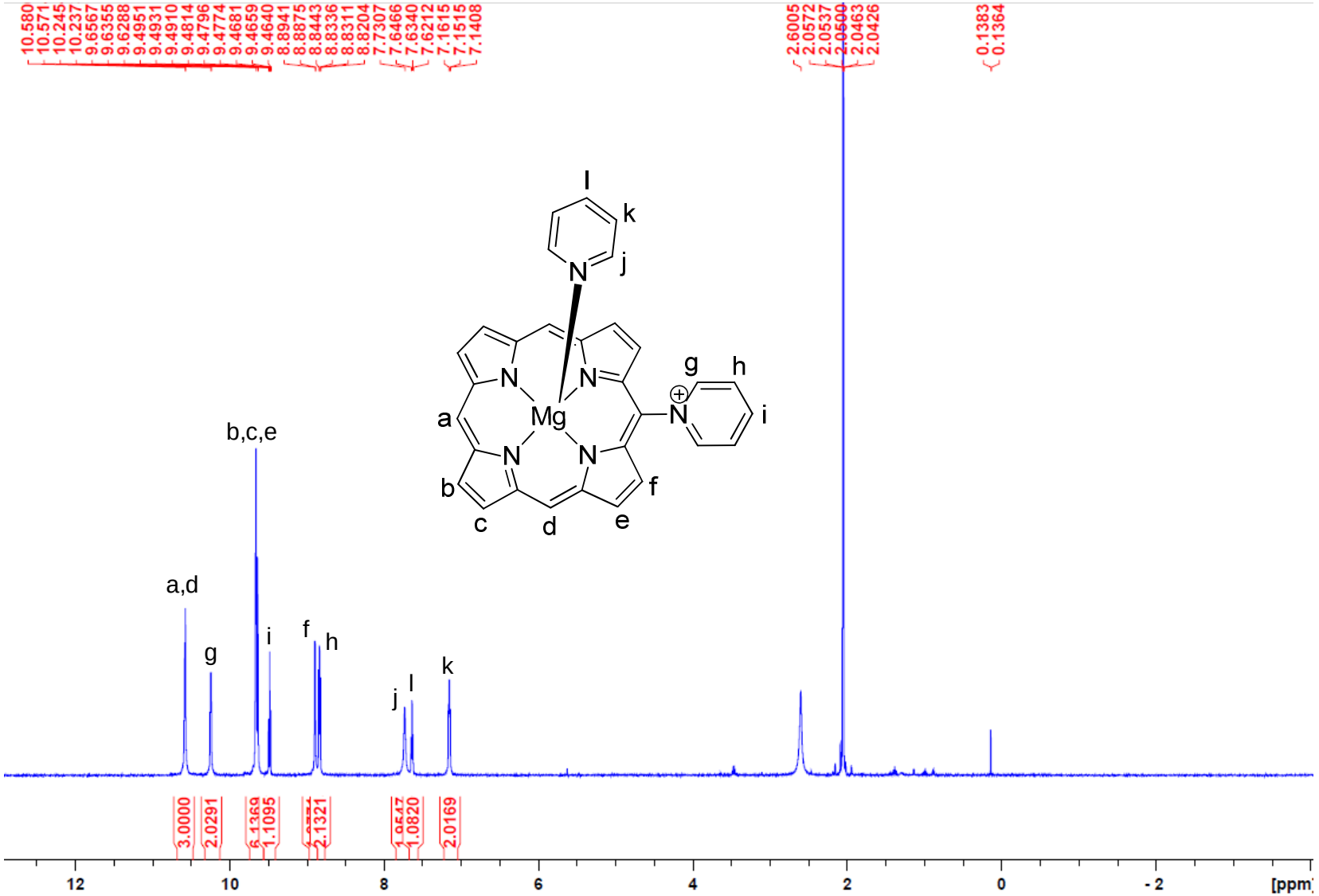

Fig. 3 ^{1}H NMR spectrum of $\mathbf{2}^{+}$,$\mathbf{PF_6}^{-}$ in CD_3COCD_3, 600 MHz, 298 K.

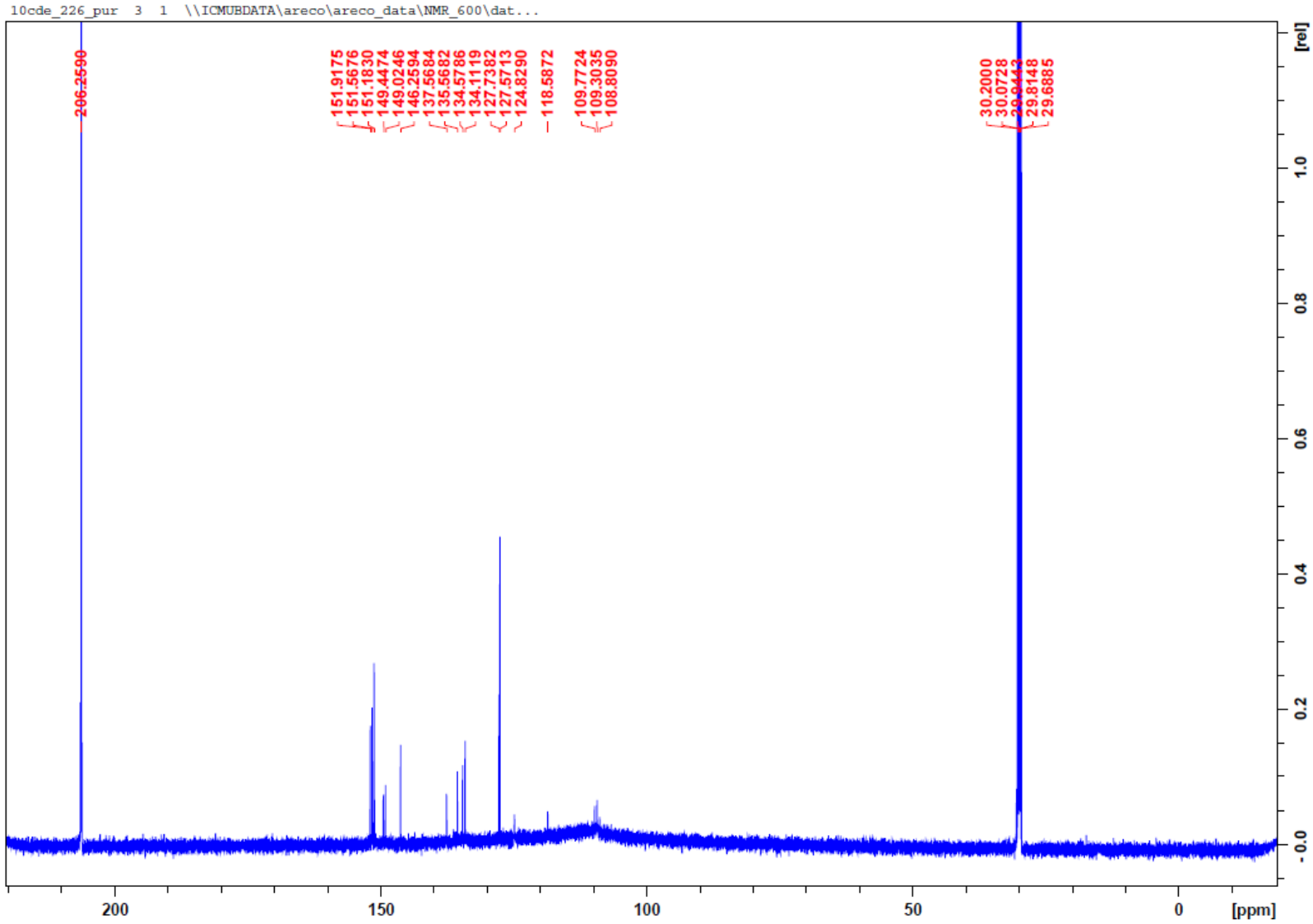

Fig. 4 ^{13}C NMR spectrum of $\mathbf{2}^{+}$,$\mathbf{PF_6}^{-}$ in CD_3COCD_3, 150 MHz, 298 K.

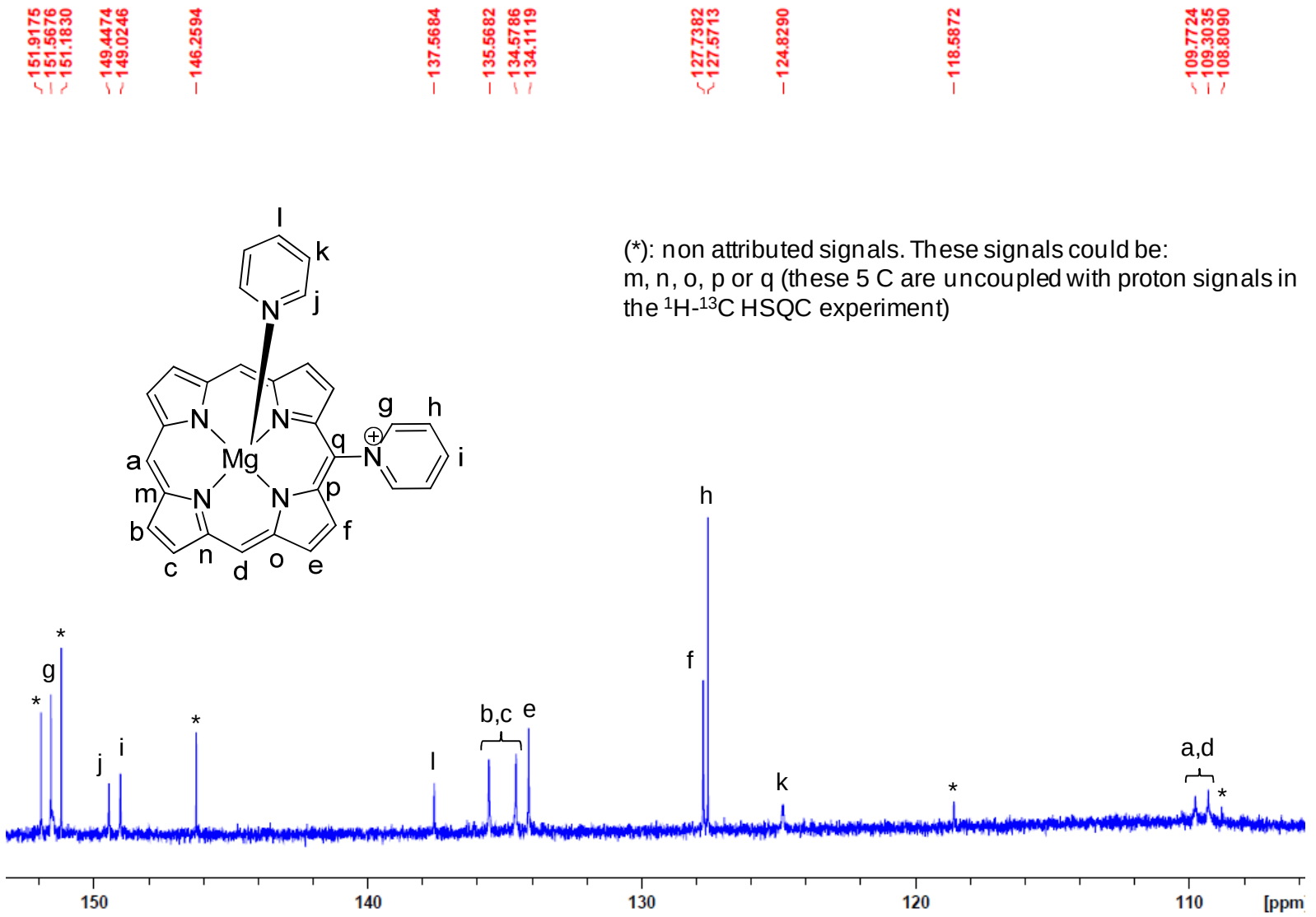

Fig. 5 Partial ^{13}C NMR spectrum of $\mathbf{2}^{+}$,$\mathbf{PF_6}^{-}$ in CD_3COCD_3, 150 MHz, 298 K.

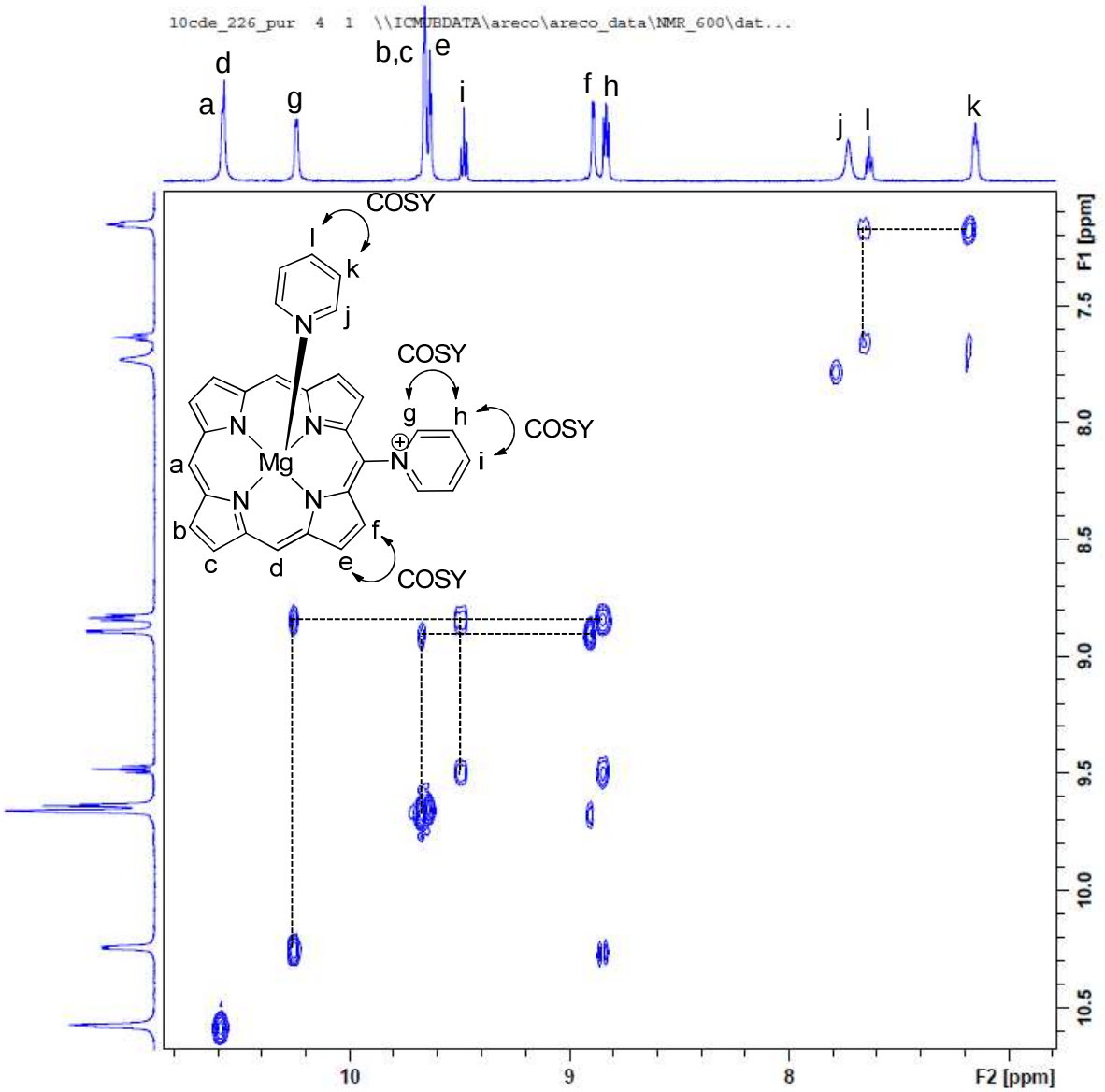

Fig. 6 ^{1}H-^{1}H COSY NMR spectrum of $\mathbf{2}^{+}$,$\mathbf{PF_6}^{-}$ in CD_3COCD_3, 600 MHz, 298 K.

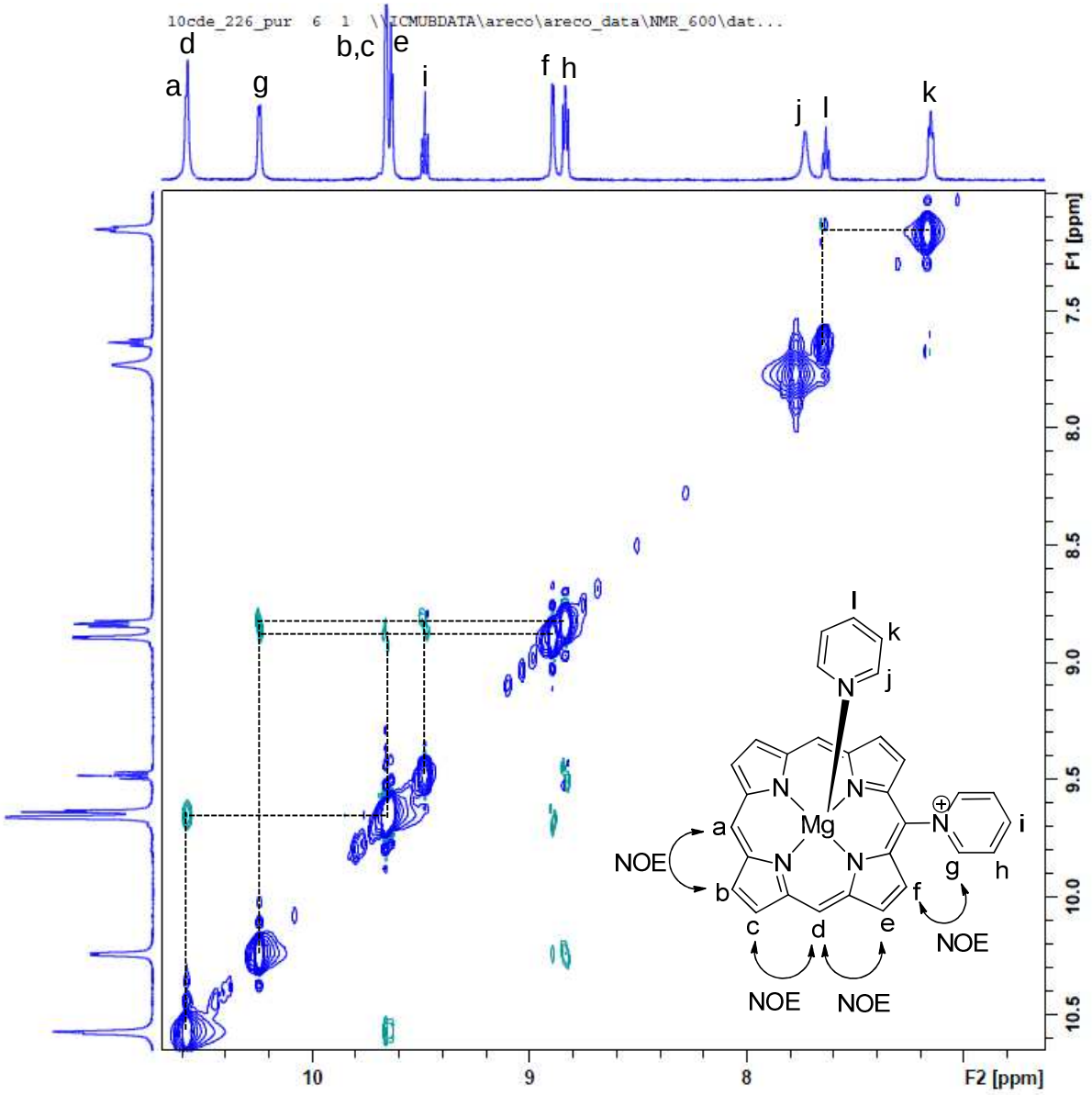

Fig. 7 ^{1}H-^{1}H NOESY NMR spectrum of **2^{+},PF$_6^{-}$·Py** in CD_3COCD_3, 600 MHz, 298 K.

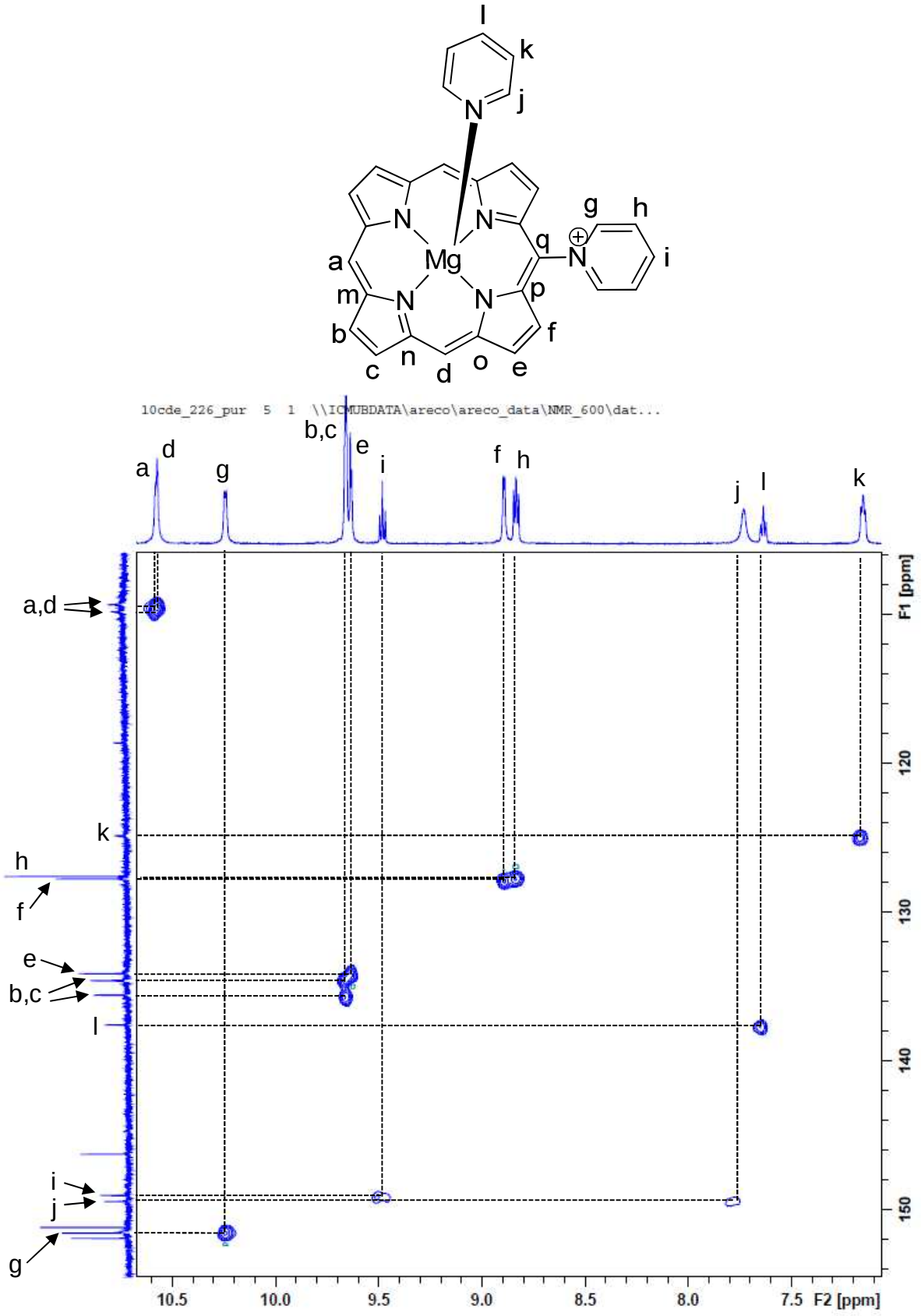

Fig. 8 ^{1}H-^{13}C HSQC NMR spectrum of $\mathbf{2}^{+}$,$\mathbf{PF_6}^{-}$ in CD_3COCD_3, 600 MHz, 298 K.

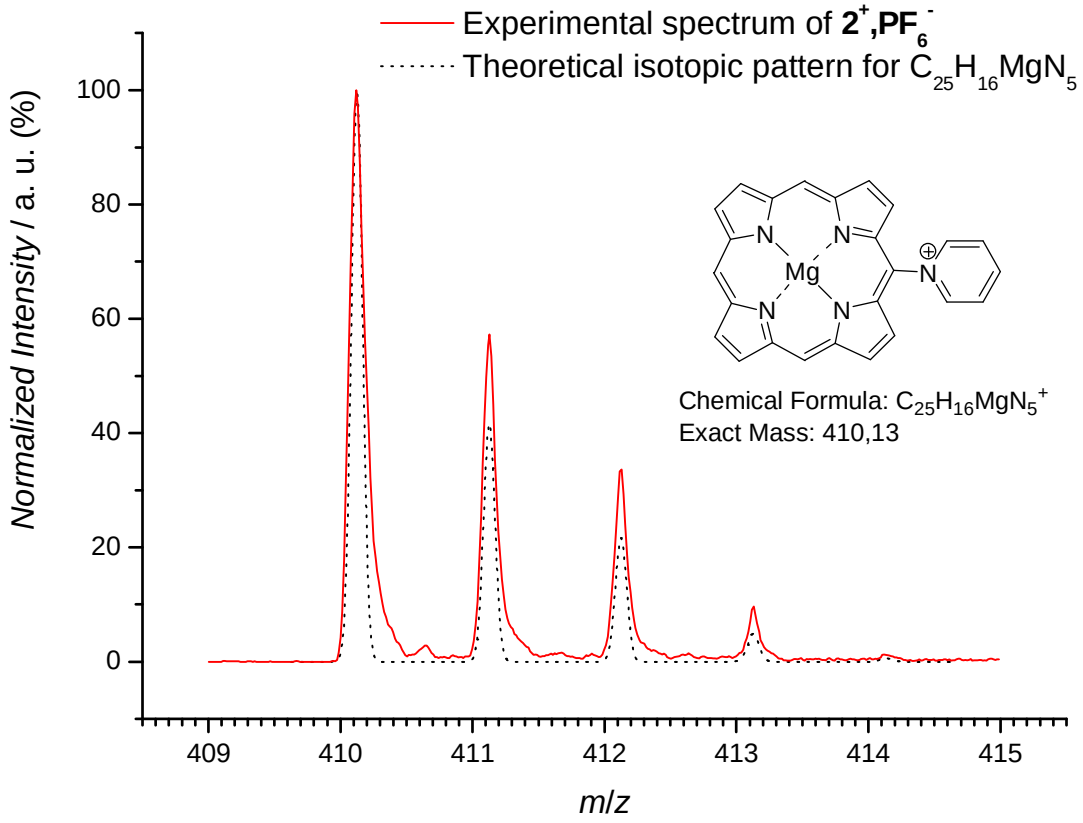

Fig. 9 Partial MALDI-TOF mass spectrum of $\mathbf{2}^{+}$,$\mathbf{PF_6}^{-}$ centered on its isotopic pattern (red/solid curve) and simulated isotopic pattern for a formula corresponding to $\mathbf{2}^{+}$ (black/dotted curve).

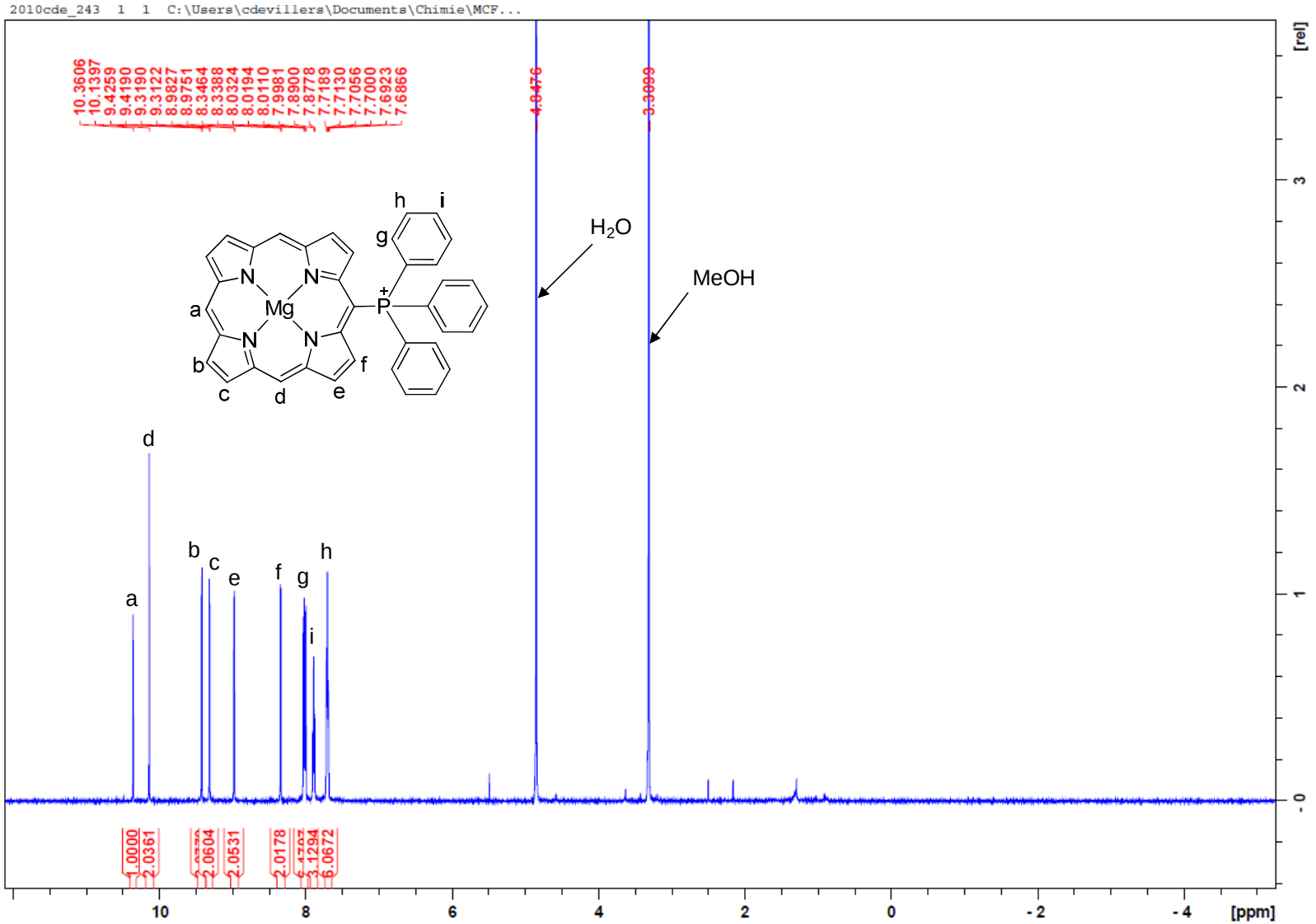

Fig. 10 ^{1}H NMR spectrum of $\mathbf{3}^{+}$,$\mathbf{PF_6}^{-}$ in CD_3OD, 600 MHz, 298 K.

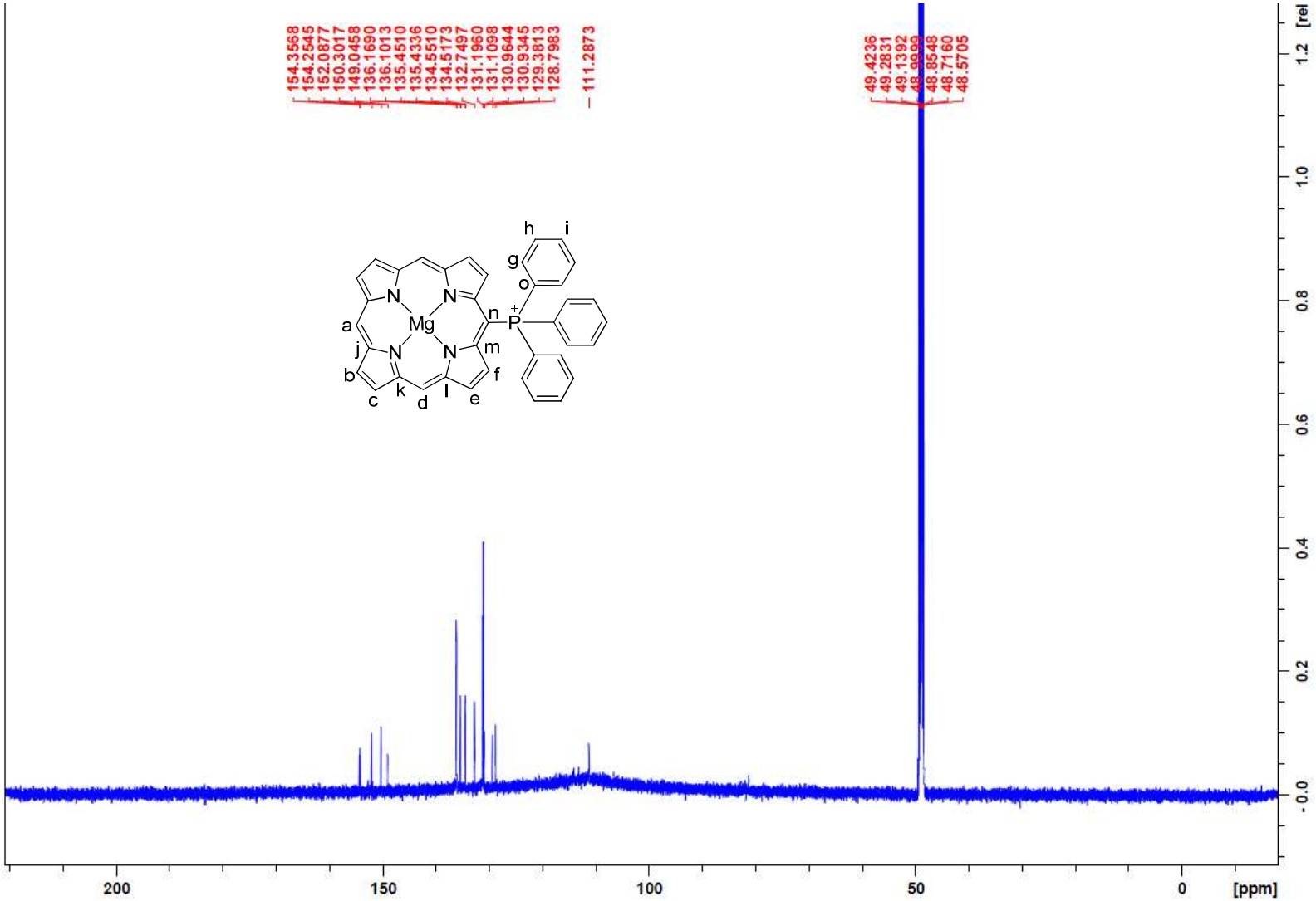

Fig. 11 ^{13}C NMR spectrum of $\mathbf{3}^{+}$,$\mathbf{PF_6}^{-}$ in CD_3OD, 150 MHz, 298 K.

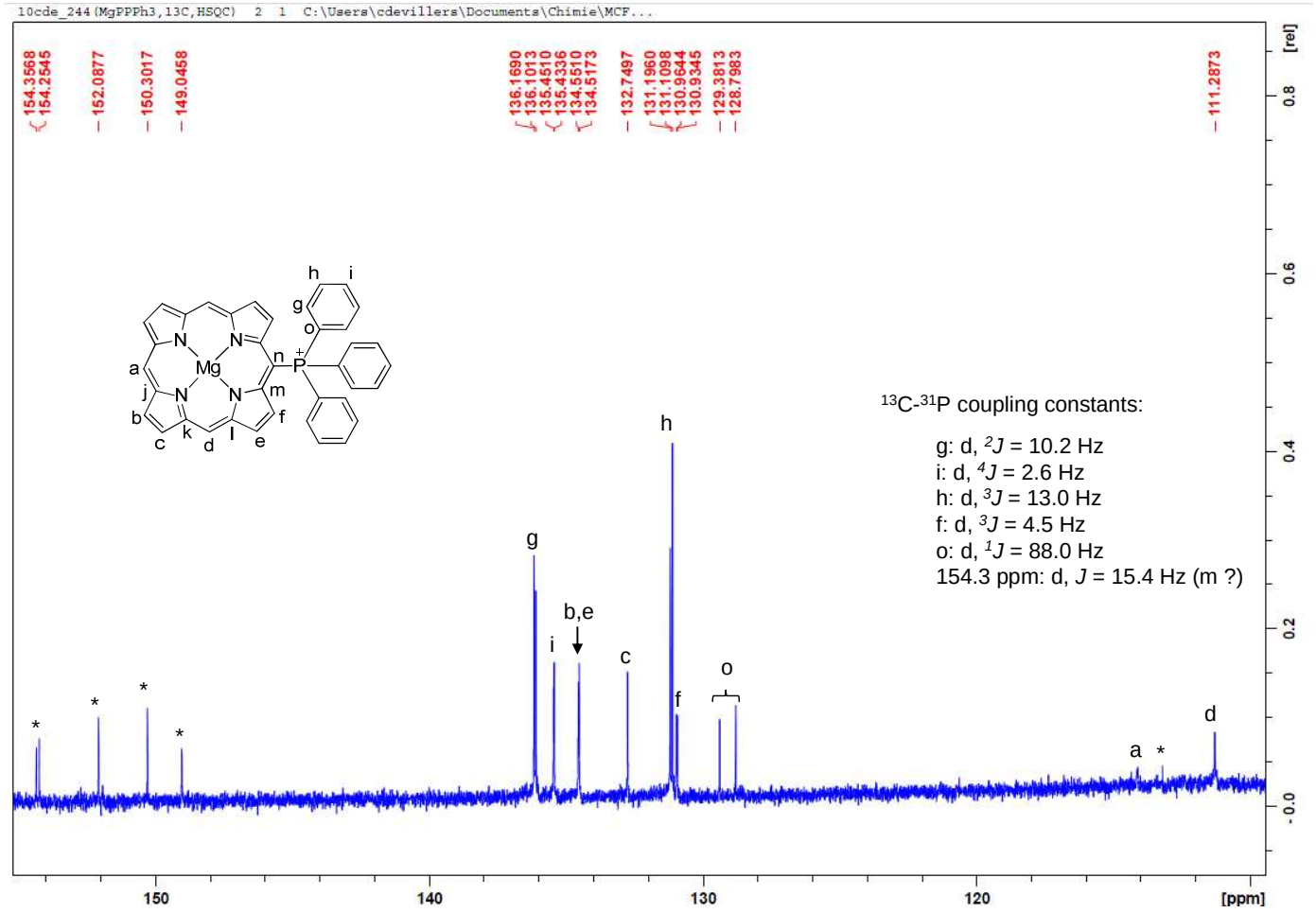

Fig. 12 Partial ^{13}C NMR spectrum of $\mathbf{3}^{+}$,$\mathbf{PF_6}^{-}$ in CD_3OD, 150 MHz, 298 K. (*): non attributed signals. These signals could be: m, l, k, j, n or o (these 6 C are uncoupled with proton signals in ^{1}H-^{13}C HSQC experiment). The "o" signal is attributed thanks to its coupling constant in comparison with phosphonium compounds reported in the literature, see for example ref [2].

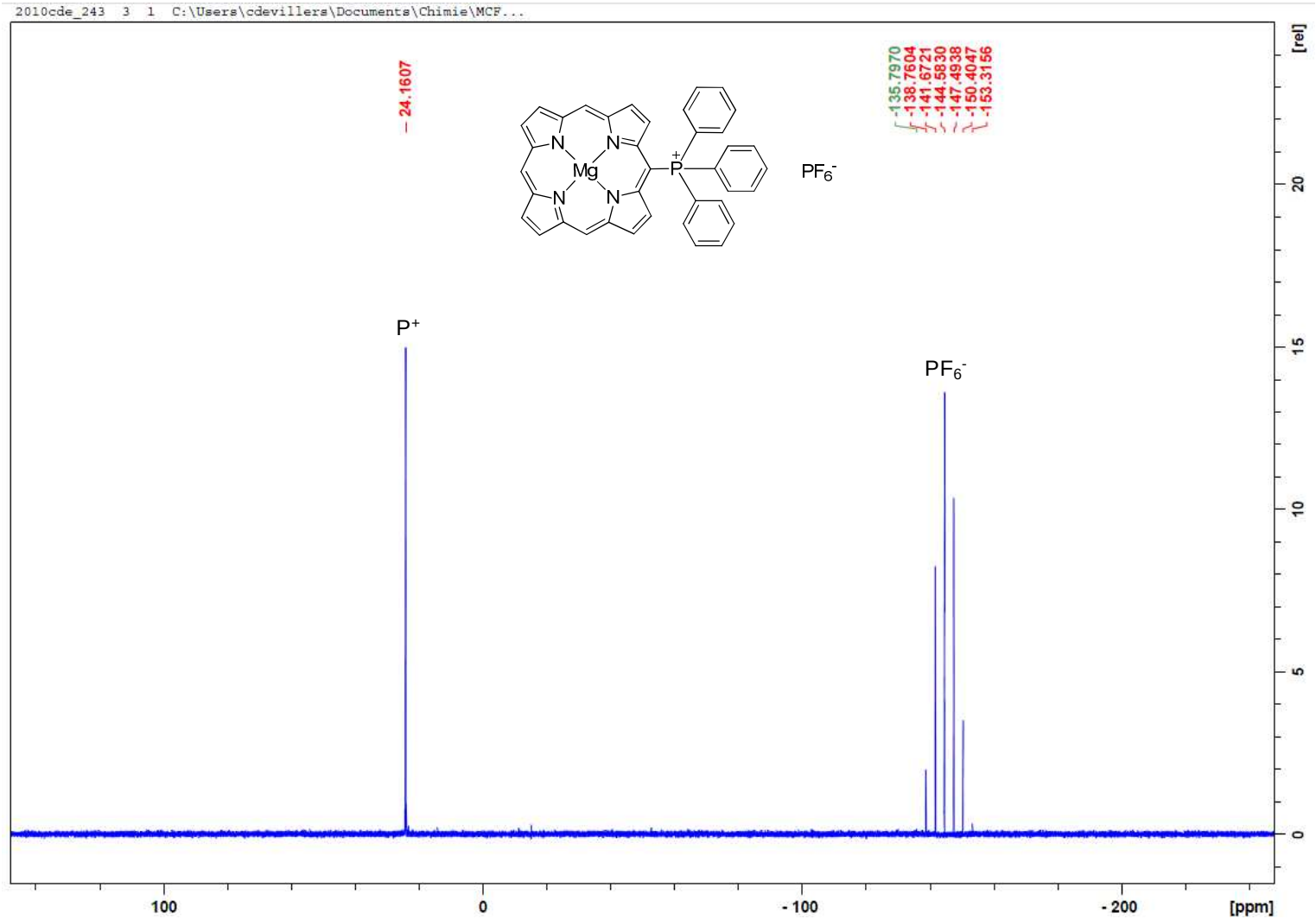

Fig. 13 ^{31}P NMR spectrum of $\mathbf{3}^{+}$,$\mathbf{PF_6}^{-}$ in CD_3OD, 243 MHz, 298 K.

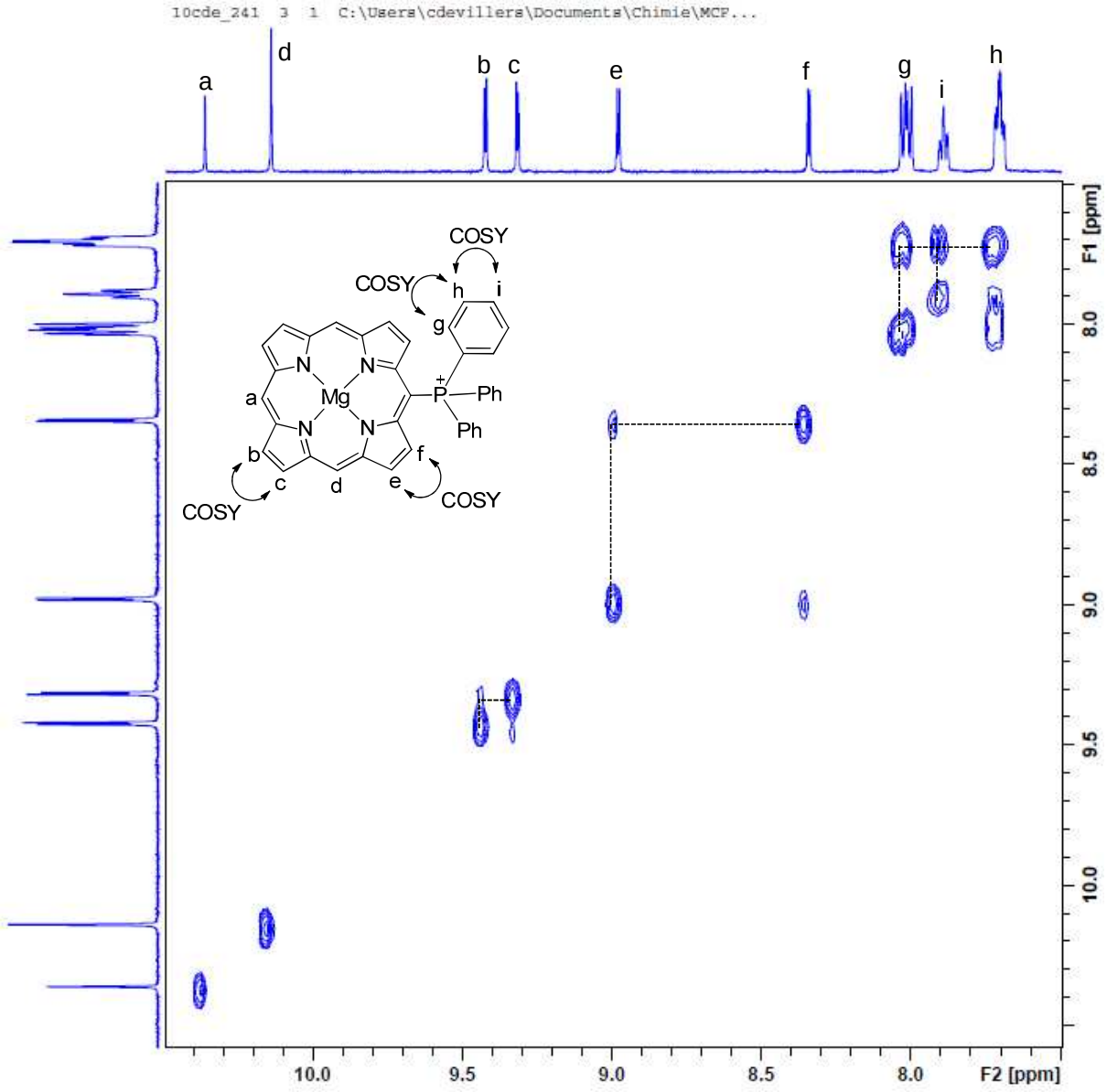

Fig. 14 ^{1}H-^{1}H COSY NMR spectrum of $\mathbf{3}^{+}$,$\mathbf{PF_6}^{-}$ in CD_3OD, 600 MHz, 298 K.

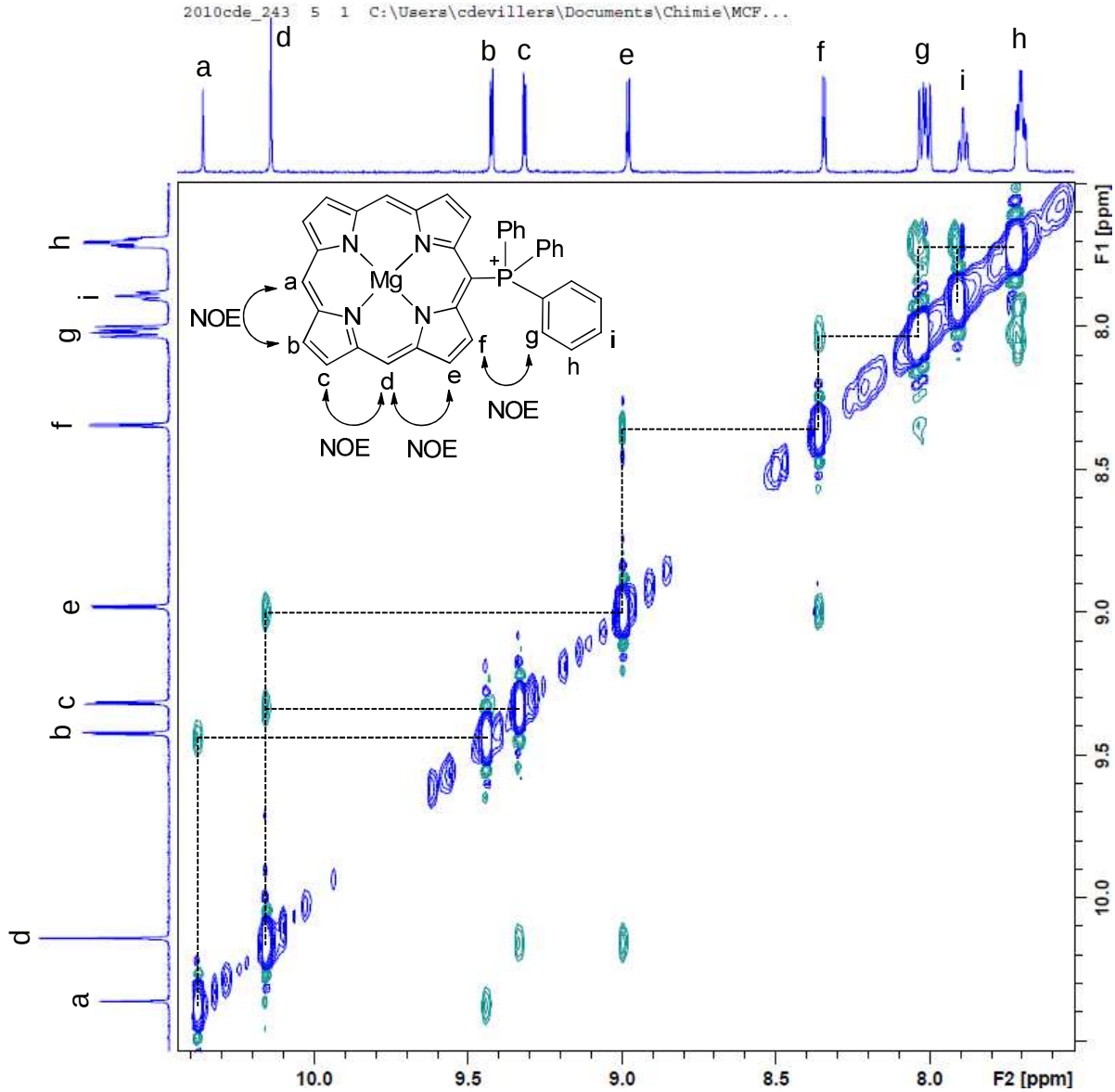

Fig. 15 ^{1}H-^{1}H NOESY NMR spectrum of $\mathbf{3}^{+}$,$\mathbf{PF_6}^{-}$ in CD_3OD, 600 MHz, 298 K.

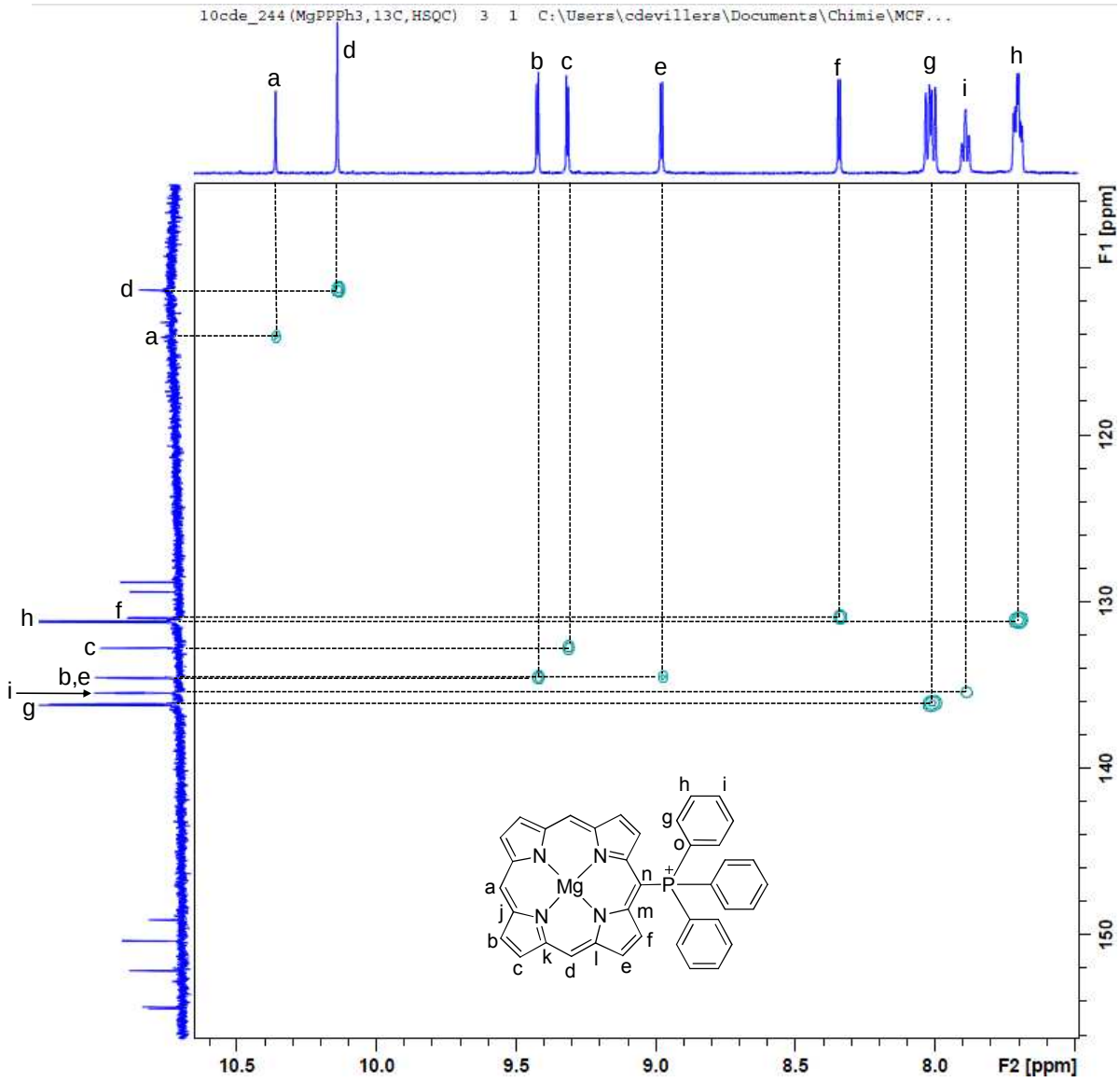

Fig. 16 ^{1}H-^{13}C HSQC NMR spectrum of $\mathbf{3}^{+}$,$\mathbf{PF_6}^{-}$ in CD_3OD, 600 MHz, 298 K.

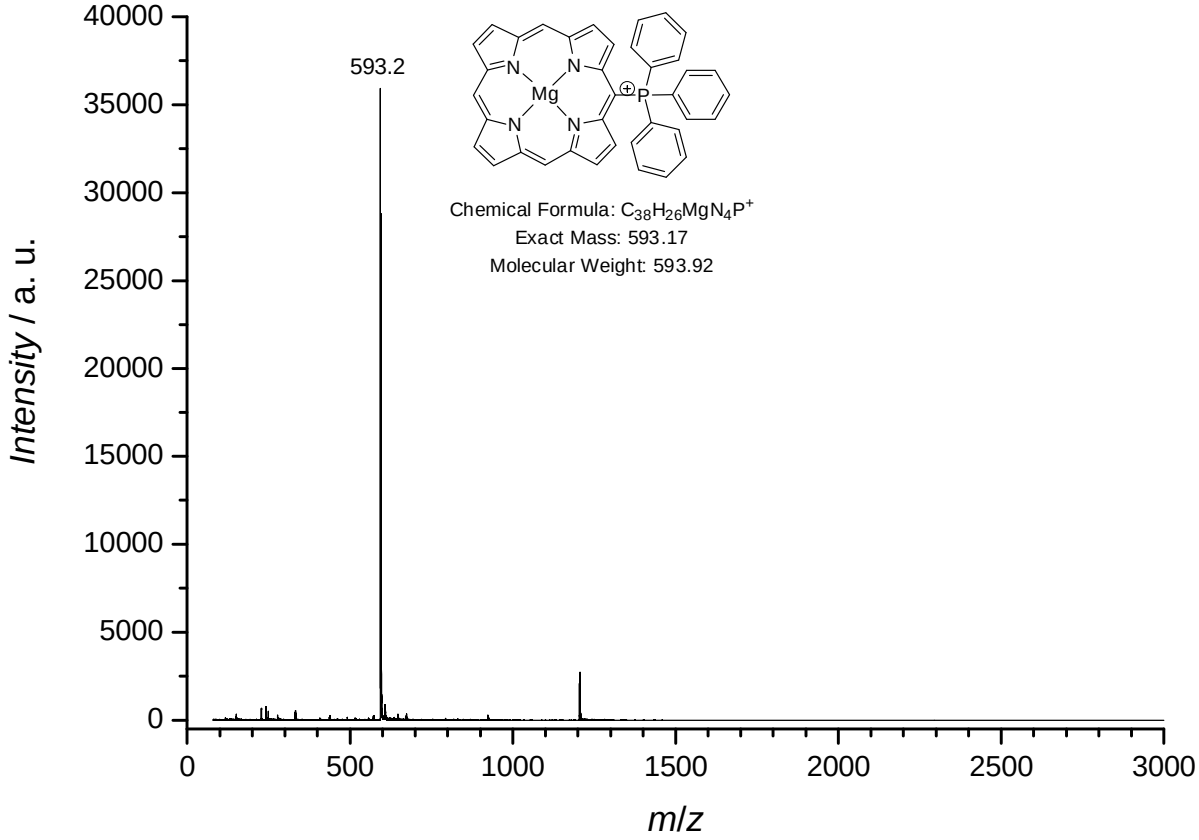

Fig. 17 MALDI-TOF mass spectrum of $\mathbf{3}^{+}$,$\mathbf{PF_6}^{-}$.

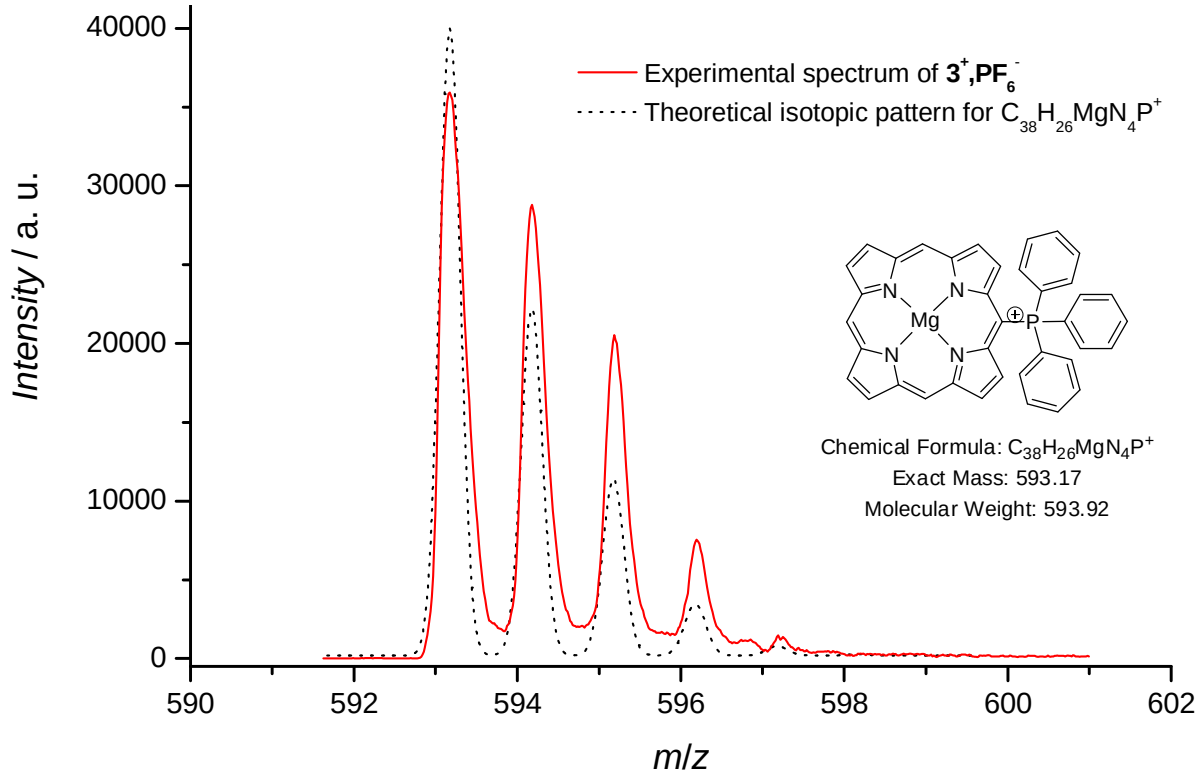

Fig. 18 Partial MALDI-TOF mass spectrum of $\mathbf{3}^{+}$,$\mathbf{PF_6}^{-}$ centered on its isotopic pattern (red/solid curve) and simulated isotopic pattern for a formula corresponding to $\mathbf{3}^{+}$ (black/dotted curve).

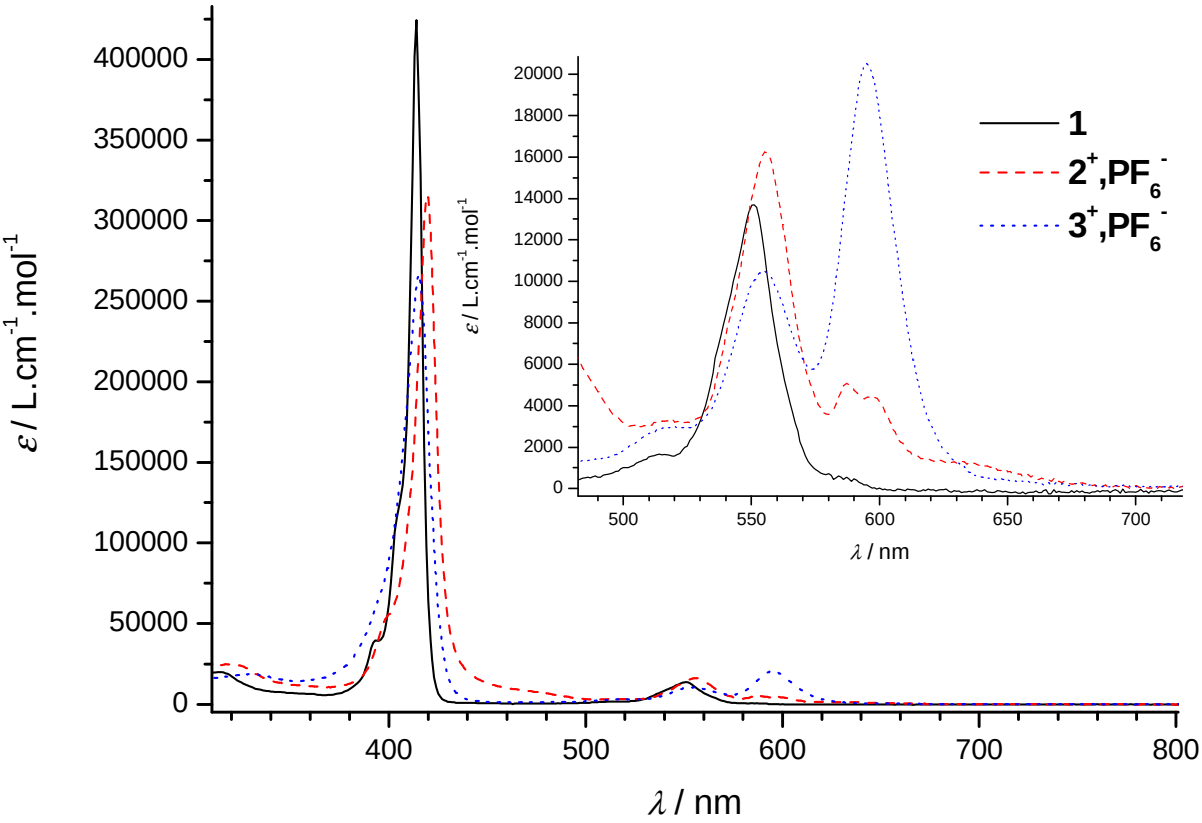

Fig. 19 UV-Visible spectra of **1** in pyridine (black/solid line), $\mathbf{2^+,PF_6^-}$ in pyridine (red/dashed line) and $\mathbf{3^+,PF_6^-}$ in CH_2Cl_2 (blue/dotted line).

References

1. D. K. Dogutan, M. Ptaszek and J. S. Lindsey, *J. Org. Chem.*, 2007, **72**, 5008.
2. E. Rémond, A. Tessier, F. R. Leroux, J. Bayardon and S. Jugé, *Org. Lett.*, 2010, **12**, 1568.